3D FLOOD INFORMATION FROM SAR AS A MEANS FOR REDUCING UNCERTAINTIES IN FLOOD INUNDATION MODELING.

Renaud Hostache[1], **Guy Schumann**[1,2], **Patrick Matgen**[1], **Christian Puech**[3], **Lucien Hoffmann**[1], **Laurent Pfister**[1]

[1] Centre de Recherche Public - Gabriel Lippmann (Dpartement EVA), L-4422 Belvaux, Grand-Duch du Luxembourg.
[2] Visiting Research Fellow, School of Geographical Sciences, University of Bristol, BS8 1SS, Bristol, UK.
[3] Cemagref (UMR TETIS), F-34093 Montpellier, France.
hostache@lippmann.lu, guy.schumann@bristol.ac.uk, matgen@lippmann.lu,
puech@teledetection.fr, hoffmann@lippmann.lu, pfister@lippmann.lu

KEY WORDS: Floods, SAR Imagery, Cartography, Distributed, Modeling, Calibration, Uncertainties.

ABSTRACT:

SAR images of river inundation prove to be very relevant for operational flood management. However, common exploitation of satellite images of floods is generally restricted to a flood extent extraction. The usefulness of these images could be significantly improved by providing a hydraulic-coherent 3-dimensional (3D) characterization of floods and by integrating these Remote Sensing-Derived (RSD) spatial characteristics of floods in hydraulic models in order to render flood inundation forecasts more reliable and accurate. This study aims at developing SAR image analysis methods that go beyond flood extent mapping in order to demonstrate the potential of these images in the spatio-temporal characterization of flood events. To fulfill this objective, two research issues were addressed. The first issue relates to water level estimation. Applied to an ENVISAT image of an Alzette River flood (2003, Grand-Duchy of Luxembourg), the developed method provides $\pm$ 54 cm average vertical uncertainty water levels, that were validated with ground surveyed high water marks. The second issue aims at evaluating how far RSD flood characteristics could allow a better constraining of hydraulic models. To achieve this goal, various calibration scenarii using only recorded hydrographs or recorded hydrographs and RSD flood characteristics are computed. These scenarii show that the integration of the RSD characteristics leads to better constrain the model (i.e. the number of parameter sets providing acceptable results with respect to observations is reduced) and render it more reliable, even in the case of quite rather abundant ground observed data.

1 INTRODUCTION AND BACKGROUND

Floods are among the most important natural hazards in the world. This explains the continuous efforts to better understand the flood generating processes and to develop strategies to reduce the damages caused by flood events. SAR images of river inundation prove to be very relevant (Schumann et al., 2007) for operational flood management. For example, the "Space and Major Disaster Charter" provides flood extent maps extracted from satellite images only a few hours after image reception. These maps are then distributed to rescue services in order to ease their operations. Especially because of their all weather image acquisition capability, Synthetic Aperture Radar (SAR) satellites are very suitable for flood extent mapping (Henry, 2004). Nevertheless, as mentioned by Smith (1997), there is no doubt that Earth observation images contain information that goes beyond simple flood extents. In this context, this paper aims at arguing that satellite images can provide 3D flood characterization and enable the constraining of uncertainties related to flood inundation modeling. Hydraulic modeling is of paramount importance in most flood forecasting and management systems. Due to huge stakes in flood management, the reliability of these flood inundation models is of primary concern (Pappenberger et al., 2005). In this framework, uncertainties need to be kept to a minimum, for example during a calibration process, using various observed data sets. Model calibration generally consists in forcing the outputs of the model so as to be as close as possible to observed data, by modifying parameter values. Nevertheless, depending on the observed data that are available, many values of parameters could allow the model to provide outputs close to observations and thus could be considered as acceptable with respect to observations. This has been introduced by Beven and Binley (1992) as the equifinality concept and induces uncertainties in the model calibration. In an operational context, the calibration is often done using point observations, such as recorded hydrographs at stream gauges. However, these data are often insufficient to make the calibration reliable (Horritt, 2000) as no reference data is available in-between these point measurements. Taking into account additional observations in calibration could help to better constrain the model, i.e. lead to a reduction of calibration uncertainties by reducing the range of acceptable parameter values (Matgen et al., 2004; Horritt, 2000; Bates, 2004).

In this context, the aim of this study is to develop methods that allow to derive 3-dimensionnal information from a SAR image of a flood in order to provide more reliable flood forecasting models. Since Schumann et al. (In Press) showed that SAR images from current satellites provide extra information only if the amount of ground point data is fairly limited, this study further aims at evaluating the advantages and the limits of taking SAR derived information into account in hydraulic modeling.

Based on the study of Raclot and Puech (2003) that provides $\pm$ 20 cm average uncertainty using aerial photographs, the water level estimation method employed here is composed of two steps (Hostache et al., 2006): i) extraction of the flood extent limits which are relevant for water level estimation, ii) estimation of water levels by merging the relevant limits and a high resolution high accuracy Digital Elevation Model (DEM) under hydraulic coherence constrains. To show the potential of satellite images for model uncertainty reduction, a stepped calibration approach has been adopted. In a first step, traditional calibration scenarii are conducted using various recorded hydrographs. In a second step, the RSD water levels are integrated in the calibration for reducing the uncertainties associated to flood inundation modeling.

2 STUDY AREA AND AVAILABLE DATA

The area of interest includes a 18 km reach of the River Alzette (Grand-Duchy of Luxembourg) between Pfaffenthal and Mersch. In this area, the River Alzette meanders in a flat plain that has an average width of 300 m (between Beggen and Mersch) and a mean slope of 0.08 %. At Mersch, the drainage area of the river Alzette covers 404 km^2. Although some large villages lie within the natural floodplain of the river, no severe damages were recorded for the early January 2003 flood (Schumann et al., 2007), which had a peak discharge of around 70.5 m^3.s^{-1} at the Pfaffenthal hydrometric station, corresponding to a return period of 5 years. With approximately 3 km.h^{-1}, the velocity of the flood peak propagation in the Alzette plain was low.

The image used in this study has been acquired by the Synthetic Aperture Radar (SAR) sensor of the ENVISAT satellite (descending orbit, C band (5.6 cm wavelength), Vertical-Vertical (VV) and Vertical-Horizontal (VH) cross polarization) at 9:57 PM, on January 2^{nd} 2003, just after the flood peak, at the beginning of the recession. This radar image, amplitude coded, has a pixel spacing of 12.5 m, resulting from the sampling of a complex image of 25 m spatial resolution. The ENVISAT image has been georeferenced using Ground Control Points (GCP) on aerial photographs. The Root Mean Squared Error (RMSE) after this georeferencing was 10 m.

The collected hydrometric data are six water stage hydrographs that were recorded at the stream gauges located in the villages of Pfaffenthal (upstream), Walferdange, Steinsel, Hunsdorf, Lintgen and Mersch (downstream). For Lintgen and Hunsdorf, recorded water stages are only available for low water depth because of measurement system disability. Moreover, the coordinates (X,Y) of 84 high water marks have been measured on the ground with a GPS ($\approx$ 5 m planimetric accuracy) and the maximum water level during the flood event has been measured using a theodolite (altimetric accuracy around $\pm$ 2 cm) at 7 points distributed across the floodplain.

The altimetric data used in this study are a LiDAR DEM (2 m spatial resolution and a $\pm$ 15 cm mean altimetric uncertainty), 200 bathymetric cross sections with a "theoretical" centimetric altimetric uncertainty (some errors of more than 30 cm have been found during ground control survey).

3 METHOD

3.1 Extraction of 3 dimensional information from SAR images

This section aims at extracting 3-dimensional information from a SAR flood image that is relevant for hydraulic modeling. In this context the methodology is composed of two steps. The first step relates to simple flood extent mapping. The innovative part in this study consists in evaluating the uncertainties in such maps and their relevance for water level estimation. The second step relates to the water level estimation. In this section, efforts will be made to evaluate the uncertainties and to remove or at least to identify the errors that are related to flood characteristics from SAR images. These efforts are necessary when the final aim is to use RSD characteristics for hydraulic model calibration. As a matter of fact, any error related to these characteristics may render the calibrated model unreliable.

3.1.1 Extraction of flood extent limits relevant for water level estimation. Flood extent mapping using SAR images is widely applied (Smith, 1997) because water appears with very low backscatter compared to other objects, thereby making flooded area detection relatively straightforward. However, in case of wind or strong precipitations that induce wavelets on the water surface, the latter could be roughened thereby increasing the backscatter. In this case, the detection of open water becomes non trivial. At the image acquisition time, the wind speed was moderate (5 m.s^{-1} recorded in a station close to the study area), causing presumably negligible wind effects on open water surfaces. In this study, radiometric thresholding has been used because it is a robust and reliable way (Henry, 2004) to detect flooded areas on SAR images. Nevertheless, although water appears with low backscatter on images, the radiometric distributions of water bodies and other land use types are not totally separated and do overlay. As a consequence, applying a single threshold value on the SAR image does not allow to detect all water bodies without detecting at the same time non flooded areas. To deal with this radiometric uncertainty, two thresholds are applied. The first one, T_{min}, aims at detecting only pixels that correspond to water bodies. As a matter of fact, the proposed value for T_{min} represents the minimum radiometric value of non-flooded pixels (i.e. outside the floodplain and outside the permanent water surfaces). The second one, T_{max}, aims at detecting all flooded areas, at the risk of detecting in addition non-flooded areas that have a similar radiometric value to the flooded one. The proposed value for T_{max} is the maximum radiometric value of water bodies outside the flooded area (i.e. lakes or the river channel if wide enough). Furthermore, although the thresholdings allow to take into account radiometric uncertainties, there remain some errors in the flood extent map that have to be corrected or at least identified in order to render the flood extent map relevant for hydraulic modeling. These errors are mainly due to shadowing effects and emerging objects that mask open water surfaces (Horritt et al., 2001).

The shadowing effects are due to hill-slopes that are not illuminated by the incident RADAR signal. They appear on SAR images with very low backscatter, similar to open water backscatter. These errors are treated by removing, using a GIS, from the flood map, areas detected as open water that are located on hill-slopes (identified using a topographic map or a DEM). The errors due to objects that mask water can not be easily corrected, but it is possible to identify objects likely to be emerged. As a consequence, the solution chosen in this study is to ignore urban and vegetated areas because they may cause highly erroneous water level estimates and to remove them from the flood extent map. This means that these areas will be given a 'No Data' value, i.e. no information about the presence or absence of water. After the treatment of error prone areas, the flood extent map has four possible values, depending on the intensity I of the SAR image pixels and the land use: 0 = certainly non-flooded ($I > T_{max}$), 1 = certainly flooded ($I < T_{min}$), 2 = potentially flooded ($T_{min} \leq I \leq T_{max}$) and 'No Data' = around buildings and trees. Then, considering that local errors in the flood extent map have been treated beforehand, pixels equal to 1 correspond only to open water and pixels equal to 0 correspond only to non open water. This induces that the potentially flooded areas (pixels equal to 2) define fuzzy limits of the flooded areas that take into account radiometric uncertainty. Moreover, the accuracy of the georeferencing of a SAR image induces additional spatial uncertainties on these fuzzy limits that need to be taken into account. To do this, it has been chosen to buffer the fuzzy limits with a size equal to the SAR image georeferencing accuracy (10 m for the ENVISAT image). The flood extent map, with buffered fuzzy limits, that represents the first result of the methodology, will be used for water level estimation.

3.1.2 Water level estimation. To derive water levels, the method is based on a merging between the fuzzy limits of the flood

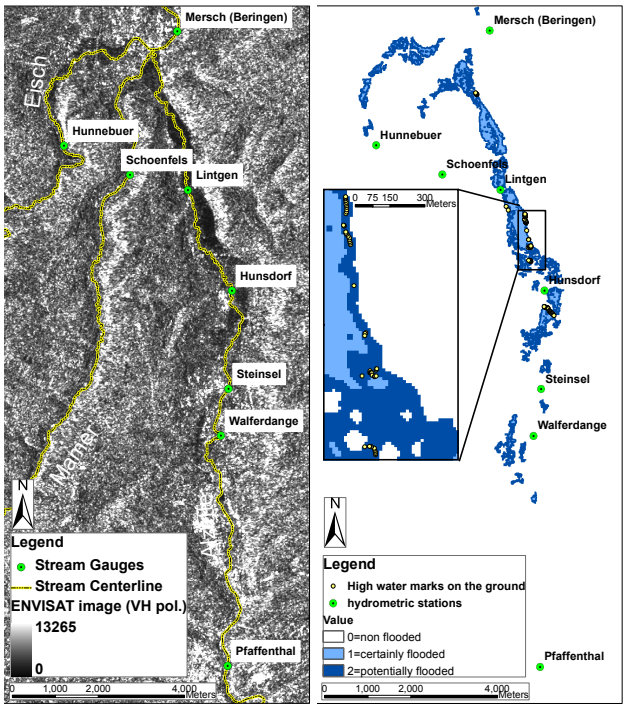

(a) (b)

Figure 1: a. Study area, ENVISAT SAR image (VH polarization, amplitude coded) and stream gauges. b. SAR image derived flood extent map.

extent map and the underlying DEM, as proposed by Brakenridge et al. (1998). As a matter of fact, during this merging, the uncertainties in the fuzzy limits are transferred to the water level estimates (Brakenridge et al., 1998; Schumann et al., submitted). Consequently, areas with gentle relief have been ignored for water level estimation because they imply important uncertainties on water level estimates. After this removal, only the most reliable limits remain. These are shaped as small patches that are sparsely distributed across the floodplain. Considering that radiometric and spatial uncertainties have been taken into account and that error prone areas have been removed beforehand, the remaining relevant limits are assumed to include the real flood extent limits (*Hyp. 1*). Under this hypothesis, the merging between relevant limits and the DEM allows the extraction of the terrain elevations inside all relevant limits and thus an estimation of intervals of water levels that should include the true value, provided that the DEM altimetric uncertainty ($unc_{DEM} = \pm 15\ cm$ for the Lidar DEM) is taken into account. This means that the intervals of water level estimation are:

$$IWL_i^{sat} = [WL_{min,i}^{sat}; WL_{max,i}^{sat}] = [El_{min,i}^{sat} - unc_{DEM}; El_{max,i}^{sat} + unc_{DEM}] \ ,$$

with $El_{min,i}^{sat}$ and $El_{max,i}^{sat}$ being respectively the minimum and the maximum values of the terrain elevation inside a given relevant limit. Then, each resulting interval of water level estimation - IWL_i^{sat} - is assumed to include the real local water level (*Hyp. 2*). However, these estimation intervals only stem from a remote sensing process and do not consider hydraulic laws governing water flow. Consequently, the water level estimation method is enhanced by a hydraulic coherence algorithm, previously developed by Raclot and Puech (2003) for water levels estimated from aerial photographs.

The hydraulic coherence algorithm is based on the law stating that water level decreases from upstream to downstream (*Hyp. 3*), in case of low flow velocity, as for the river Alzette. To apply *Hyp. 3* to the remotely sensed water levels IWL^{sat}, the flow directions between locations of water level estimates need to be known. For hydraulic modeling, a one-dimensional (1D) model has been developed. This model is based on the assumption of 1D hydraulic flow. This means that the water flows from one cross section to the following starting at the first cross section (upstream boundary condition) and ending at the last one (downstream boundary condition) (Roux and Dartus, 2006). Using the same flow scheme on the relevant limits, it has been possible to determine a hydraulic hierarchy, composed of up-/downstream relationships between locations of water level estimation - corresponding to the locations of the relevant limits. Thus, *Hyp. 3* means that if the relevant limit A is upstream of the relevant limit B, then the water level must decrease from A to B. Due to *Hyp. 2*, the hydraulic coherence algorithm may force the following constraints: $WL_{max}^{sat}(B) \leq WL_{max}^{sat}(A)$, and vice-versa $WL_{min}^{sat}(A) \geq WL_{min}^{sat}(B)$. As a consequence, propagating these constraints following the flow direction, the algorithm forces a decrease upon the maxima ($WL_{max,i}^{sat}$) from upstream to downstream and a rising upon the minima ($WL_{min,i}^{sat}$) from downstream to upstream. This provides constrained water level estimates, called final water levels hereafter, that will be integrated in the calibration process.

3.2 Introduction of remote sensing-derived flood characteristics to the hydraulic model calibration

The aim of the second part of the methodology is to better constrain the hydrodynamic model using the RSD spatially distributed water levels. Recent studies (Bates, 2004; Matgen et al., 2004) have shown that flood extents derived from SAR images could be useful for hydraulic model calibration. The originality in this study is to integrate a different kind of information derived from SAR, namely water levels. To deal with uncertainties in the observed data and the parameter value determination, the calibration process has been based on Monte-Carlo simulations.

3.2.1 Hydraulic model structure. The set up of a hydraulic model requires the knowledge of a three-dimensional (3D) geometry of the floodplain and channel, initial conditions, boundary conditions and hydraulic parameters, e.g. friction coefficients. For a one dimensional (1D) hydraulic model, the geometry is defined by a main flow line - usually the median axis of the river channel (Roux and Dartus, 2006), and cross sections, placed perpendicularly to the main flow line. In 1D modeling, it is assumed that the water level is uniform on each cross section. The hydraulic model used in this study has been set up under Hec-RAS (United States Army Corps of Engineers (USACE), 2002). The 3D geometry of the model has been extracted using the DEM and the bathymetric data (Cf. section 2). The upstream boundary condition is the discharge hydrograph calculated at the Pfaffenthal hydrometric station using the recorded stage hydrograph and a rating curve (relationship between water depth and discharge), and the downstream boundary condition using the rating curve at the Mersch hydrometric station (Figure 1). Furthermore, an inflow has been imposed 2 km upstream of Mersch as the discharge hydrograph calculated using the rating curves and the limnigraphs recorded at Schoenfels (River Mamer) and Hunnebuer (River Eisch) stream gauges (Figure 1). The initial condition is calculated by the model as a steady flow simulation using the discharge at the Pfaffenthal hydrometric station (upstream boundary) at the starting time. The calibration parameters are two Manning friction coefficients (one for the river channel and one for the floodplain). A single channel Manning coefficient has been attributed for the entire reach in the model because the channel aspect appeared homogeneous along the study area during field observations. Moreover, the aim is to avoid over-parameterization and to focus on the interest of taking RSD water

levels into account during calibration. Additionally, with friction inside the floodplain being higher than inside the riverbed, the Manning coefficient in the floodplain should be higher than that of the channel.

3.2.2 Calibration process. The aim of a calibration is to find the parameter values that enable the model to provide outputs that are close to observations. If no satisfactory results can be obtained with any of the tested parameter sets, the model assumptions, the model structure and the boundary conditions should be questioned (Beven and Binley, 1992). The calibration process used in this study is based on a random generation of parameter sets and subsequent hydraulic model simulations with each set of parameters. Subsequently, outputs provided by each simulation are compared to recorded observations. Using this calibration process, it is possible to represent performances of the model versus parameter values (Horritt, 2000).

In this study, as proposed by the GLUE methodology (Beven and Binley, 1992), the uncertainty of the observations is taken into account during the model performance calculation. This means that the outputs of the model are compared with the observation using fuzzy logic: each point observation data is affected by an interval representing the measurement uncertainty. As a matter of fact, the simulated water levels are compared with intervals of observed water levels. For the RSD water levels, the estimations are obtained directly as intervals ($IWL_{sat}^{obs} = [WL_{min}^{obs}; WL_{max}^{obs}] = [WL_{min}^{sat}; WL_{min}^{sat}]$) that take uncertainties into account. For water levels recorded at stream gauges WL^{obs}, it has been assumed that the measurement uncertainty is around $\pm$ 1 cm:

$$\begin{aligned} IWL_{stream}^{obs} &= [WL_{min}^{obs}; WL_{max}^{obs}] \\ &= [WL_{stream}^{obs} - 0.01; WL_{stream}^{obs} + 0.01] \end{aligned}$$

To evaluate the model results, the RMSE has been used in this study because it allows the calculation of a global performance criterion that combines various kinds of water level observations.

$$\begin{gathered} RMSE = \sqrt{\sum_{t,x} \frac{\Delta WL^2}{n}} \\ \text{with: } \Delta WL = \\ \left\{ \begin{array}{c} 0 \text{ if } WL^{sim} \in \left[WL_{min}^{obs}; WL_{max}^{obs}\right] \\ WL^{sim} - WL_{min}^{obs} \text{ if } WL^{sim} < WL_{min}^{obs} \\ WL^{sim} - WL_{max}^{obs} \text{ if } WL^{sim} > WL_{max}^{obs} \end{array} \right\} \end{gathered} \quad (1)$$

In (1), WL_{sim} is the simulated water level at time t and at cross section x, n is the number of observed water levels used for the RMSE calculation, and WL_{min}^{obs} and WL_{max}^{obs} are the bounds of the intervals of observed water levels as defined previously. With this definition, the RMSE gives the same weight to each observed water level (in time and space).

Previous studies (Hostache et al., 2007; Schumann et al., In Press) have shown that RSD flood information is useful to reduce uncertainties in case of limited calibration data. In this study, the aim is to evaluate how far RSD flood information is useful for uncertainty reduction in hydraulic model calibration with more abundant calibration data. If many stream gauges are available, we propose to address various calibration scenarii to evaluate the enhancement provided by the integration of RSD water levels. This means that every possible combination of one, two and so on stream gauges (6 available at maximum for the Alzette study area) is used to calculate a RMSE of the model results with and without taking into account the RSD water levels. In each calibration scenario, using the RMSE to assess model performance, the simulated water levels are compared with the observed water levels (1). For example, if two stream gauges S_1 and S_2 and RSD water levels are available, six scenarii are addressed, providing six RMSE values: RMSE(S_1), RMSE($S_1 \cup RSD$), RMSE(S_2), RMSE($S_2 \cup RSD$), RMSE($S_1 \cup S_2$), RMSE($S_1 \cup S_2 \cup RSD$).

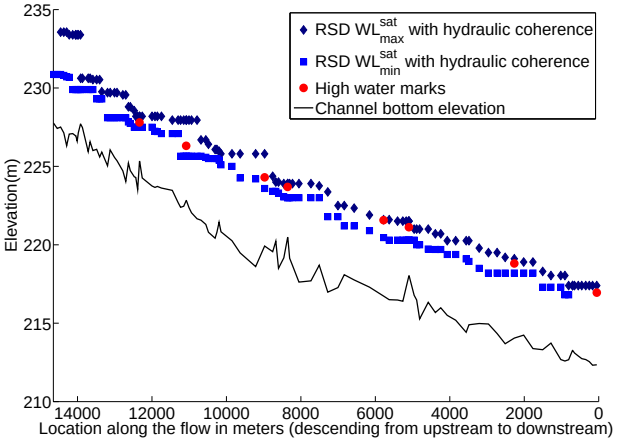

Figure 2: Remote Sensing-Derived water levels and ground surveyed high water marks.

4 RESULTS AND DISCUSSION

4.1 Water level estimation

To extract the flood extent, a double thresholding has been applied to the georeferenced ENVISAT image (VH polarization) (Figure 1 a). The thresholding of the SAR image using T_{min} and T_{max} provides the flood extent map shown in Figure 1 b. As partial validation of the RSD flood boundaries, ground surveyed high water marks (yellow dots) located in areas without trees or buildings have been added to Figure 1 b. 92 % of these are included in the fuzzy limits of the flood extent map. Moreover, the mean distance between the high water marks that lie outside the fuzzy limits and these fuzzy limits is equal to 4 m. This is lower than the coordinate accuracy of these points (accuracy of the GPS used to calculate the high water marks is of approximately 5 m). As a consequence, these results show that the method employed in this study for flood extent mapping is suitable. Hence, the *Hyp. 1* and the assumption of low wind effects on water surface roughness are appropriate.

As the limits of the flood extent map are fuzzy, the water level estimates resulting from the merging between these limits and the DEM are in the form of intervals. To characterize the uncertainty of the resulting initial water level estimates, the half mean interval ($\frac{mean(WL_{max}^{sat} - WL_{min}^{sat})}{2}$) of the resulting water level estimates has been calculated. This "mean uncertainty", equal to $\pm$ 88 cm, is relatively high. Then, the constraining algorithm of initial water level estimates using hydraulic coherence concepts has been applied. This provides final water level estimates shown in Figure 2 with a mean uncertainty (see above) of $\pm$ 54 cm. Compared to the mean uncertainty of the initial RSD water levels ($\pm$ 88 cm), this value shows a significant improvement and thus a better capability of the final water levels to reduce the uncertainties of a hydraulic model can be expected. Moreover, Figure 2 shows that each *in situ* high water mark measurement is included in the corresponding interval of RSD water level, which is crucial because it validates at least partially the RSD water levels and especially *Hyp. 2* which states that the "true" water level is inside the intervals of RSD water levels.

4.2 Evaluation of hydraulic model calibration uncertainty reduction by the means of remote sensing-derived water level integration

The calibration of the hydraulic model was based on Monte-Carlo simulations. For this procedure, 2000 sets of parameters were randomly generated within the following intervals of physically plausible values: $n_c \in [0.01; 0.1]$ and $n_{flp} \in [0.01; 0.2]$ for the channel and floodplain Manning coefficients respectively. Next, for each generated set of parameters, one hydraulic model run (between the 1^{st} of January 2003, at 03:00 PM, and the 8^{th} of January 2003, at 00:00 AM) was performed, and the results of these simulations were compared with observations by calculating an RMSE (1). To estimate the acceptable values of the model parameters, those providing the lowest RMSE, with a tolerance of $\pm$ 1 cm (i.e. RMSE $\approx$ RMSE $\pm$ 1 cm) have been selected. This tolerance is reasonable considering that a 1 cm decrease of the RMSE does not represent a significant enhancement of the model results.

On the reach between Pfaffenthal and Mersch, water stage hydrographs are available at six stream gauges (Figure 1 a). For each combination of one to six of these stage hydrographs, a RMSE (1) between the recorded and simulated water stages has been calculated. Next, the same calculations have been done by adding the RSD water levels in order to evaluate the performance gain given by these RSD flood characteristics. Using these RMSE, it is possible to obtain, for each of these calibration scenarii, a set of acceptable values of model parameters. To estimate the calibration uncertainty, two indicators have been chosen. The first one is the range of acceptable parameter values (n_c and n_{flp}). The second one is the average deviation between the maximum and the minimum values of the water levels simulated by the set of acceptable models (mean WS deviation). This second indicator provides an average uncertainty (in meters) on the water levels simulated by the acceptable model ensemble. Furthermore, to estimate the reliability of the acceptable model ensemble, the indicator chosen is the global RMSE between the simulated water levels and all available observations of water level (the six water stage hydrographs, the RSD water levels and the ground surveyed high water marks). This provides the mean error of the water levels predicted by the acceptable model ensemble. Table 1 and Table 2 summarize the results of the calibration process for each calibration dataset. In Table 1, only the water stage hydrographs are used for the calibration. In this table, the values have been calculated by averaging the indicators proposed above for each calibration scenario that takes a given number (1 to 6) of stage hydrographs into account. Table 2 shows the same indicators, but calculated for the calibration scenarii that take into account stage hydrographs recorded at stream gauges and RSD water levels.

In Table 1 and Table 2, although the acceptable values of the channel Manning coefficients seem higher than expected for such a river, the ensembles of acceptable parameters obtained in this study are in agreement with those obtained by Schumann et al. (2007) for a similar reach of the river Alzette. This could be due especially to the presence of trees on the stream embankments that increase the frictions for the overtopping water. Moreover, it is worth noting that the ranges of acceptable floodplain Manning coefficients are large. A simple reason is that this flood event is of relatively low magnitude (5 year return period), which induces that most of the water (more than 90 % in this case) flows through the channel.

Additionaly, contrary to what could be expected, the most constrained intervals of acceptable parameters are not obtained when the maximum number of water stage hydrographs is taken into account in the calibration. For example, scenario 2 in Table 2 (i.e. 2 hydrographs and RSDWL) gives a more constrained interval than scenario 6 (6 hydrographs and RSDWL). This is due to the 1 cm variation around the minimum RMSE that has been allowed to determine the acceptable set of parameters. As a matter of fact, the threshold for the model parameter set acceptability changes from one scenario to the other. Therefore, it is possible that the liberty with 6 gauges is more important than with 2 due to the fact that the optimal parameter set is not the same for each water stage hydrograph.

Table 1 and Table 2 show that the integration of RSD water levels allows a reduction of acceptable parameter value ranges. This induces a significant reduction of the model results uncertainty considering that the decrease of the simulated water stage mean deviation is equal to 7-10 cm if the RSD water levels are integrated in the calibration. Even if the reduction of uncertainty becomes lower when considering a higher number of hydrographs, it is significant. As a consequence, Table 1 and Table 2 illustrate a significant enhancement of the calibration when integrating the RSD water levels. Moreover, in all scenarii, the global RMSE, which is an indicator of the calibrated model accuracy, is a little reduced by the integration of the RSD water levels. This means that the RSD flood information tends to render the model more reliable and accurate.

Calibration dataset	Uncertainty/Accuracy			
	ranges of acceptable parameter values		mean WS deviation (m)	global RMSE (m)
	n_c	n_{flp}		
1 WS Hy.	0.046-0.052	0.05-0.2	0.15	0.24
2 WS Hy.	0.046-0.052	0.05-0.2	0.15	0.23
3 WS Hy.	0.046-0.053	0.05-0.2	0.17	0.22
4 WS Hy.	0.046-0.053	0.05-0.2	0.17	0.22
5 WS Hy.	0.047-0.054	0.05-0.2	0.18	0.22
6 WS Hy.	0.047-0.054	0.05-0.2	0.18	0.22

Table 1: Uncertainty and accuracy for the calibration scenarii based only on water stage hydrographs (WS Hy.).

Calibration dataset	Uncertainty/Accuracy			
	ranges of acceptable parameter values		mean WS deviation (m)	global RMSE (m)
	n_c	n_{flp}		
1 WS Hy. + RSD WL	0.048-0.05	0.11-0.18	0.05	0.23
2 WS Hy. + RSD WL	0.049-0.051	0.06-0.2	0.05	0.22
3 WS Hy. + RSD WL	0.048-0.051	0.05-0.18	0.1	0.22
4 WS Hy. + RSD WL	0.048-0.052	0.05-0.18	0.09	0.22
5 WS Hy. + RSD WL	0.048-0.052	0.05-0.18	0.1	0.22
6 WS Hy. + RSD WL	0.048-0.052	0.05-0.17	0.1	0.22

Table 2: Uncertainty and accuracy for the calibration scenarii based on water stage hydrographs and RSD water levels.

5 CONCLUSIONS AND FUTURE WORK

Smith (1997) and Raclot and Puech (2003) argued that potential exploitations of flood images go beyong simple flood extent mapping. In this context, previous studies succeeded in estimating water levels using a merging between SAR images of floods and DEM, but with important uncertainties (1-3 m for Brakenridge

et al. (1998)) or with good accuracy (Schumann et al., 2007) but uncertainties difficult to assess (Schumann et al., submitted). In this framework, the methodology presented in this study allows the estimation of water levels with associated uncertainty bounds, accurately enough to reduce uncertainties in a hydraulic model calibration. The RSD water level estimates have been obtained with a $\pm$ 54 cm mean uncertainty, using an ENVISAT SAR image of a River Alzette flood event. This water level estimation presents a lower uncertainty than the one observed by Brakenridge et al. (1998). This is due to an analysis of the hydraulic relevance of RSD flood extents and a hydraulic coherence algorithm, previously developed by (Raclot and Puech, 2003) for arial photographs. Although the uncertainty is higher in the current study than in the study of Raclot and Puech (2003) (uncertainty $\approx \pm$ 20 cm), satellite imagery offers enhanced potential to obtain RSD water levels that are accurate enough to be useful in hydraulic model calibration.

Integrated in a hydraulic model during calibration in addition to traditional calibration data -e.g. water stage hydrographs-, the RSD water levels are capable of significantly reducing uncertainties - i.e. by reducing the ranges of acceptable parameter values, even in the case of quite rather abundant ground observed data. Indeed, for a 1-D model of the river Alzette, integrating the RSD water level in the calibration complementary to six water stage hydrographs distributed along the river bed, the reduction of the uncertainty on the simulated water levels is equal to 7 cm. This result shows the efficiency of the RSD water levels for reducing calibration uncertainty. As a consequence, using the methodology presented in this study, the predictions of the calibrated model become more suitable due to a better constraining, both temporally and spatially.

Furthermore, with the launch of new radar satellites (e.g. ALOS, RADARSAT-2, Cosmo-Skymed, TerraSar-X) that have better spatial and radiometric resolutions, the uncertainties of water level estimates will presumably be further reduced, getting closer to the results of Raclot and Puech (2003) obtained with aerial photographs. Moreover, in addition to the use of RSD water levels for calibration, it would be of great interest to evaluate the possibilities of assimilating such data in hydraulic models (Matgen et al., 2007), since this may allow the forecasting of flood extents with a higher accuracy.

ACKNOWLEDGEMENTS

This study has been partially funded by the National Research Fund (FNR) of Luxembourg through the VIVRE program (FNR / VIVRE / 06 / 36 / 04), and the Belgian Science Policy Office in the framework of the STEREO II program - project SR/00/100.

REFERENCES

Bates, P., 2004. Remote sensing and flood inundation modelling. *Hydrological Processes* 18(13), pp. 2593–2597. 1, 3

Beven, K. and Binley, A., 1992. The future of distributed models - model calibration and uncertainty prediction. *Hydrological Processes* 6(3), pp. 279–298. 1, 4

Brakenridge, G. R., Tracy, B. T. and Knox, J. C., 1998. Orbital SAR remote sensing of a river flood wave. *International Journal of Remote Sensing* 19(7), pp. 1439–1445. 3, 5, 6

Henry, J.-B., 2004. Spatial information system for floodplain inundation risk management (In French : Systèmes d'information spatiaux pour la gestion du risque d'inondation de plaine). PhD thesis, Strasbourg I University, France. 1, 2

Horritt, M. S., 2000. Calibration of a two-dimensional finite element flood flow model using satellite radar imagery. *Water Resources Research* 36(11), pp. 3279–3291. 1, 4

Horritt, M. S., Mason, D. C. and Luckman, A. J., 2001. Flood boundary delineation from synthetic aperture radar imagery using a statistical active contour model. *International Journal of Remote Sensing* 22(13), pp. 2489–2507. 2

Hostache, R., Puech, C., Schumann, G. and Matgen, P., 2006. Estimation of water levels in a floodplain with satellite radar images and fine topographic data (In French: Estimation de niveaux d'eau en plaine inondée à partir d'images satellites radar et de données topographiques fines). *Remote Sensing Journal (In French: Revue Télédétection)* 6(4), pp. 325–343. 1

Hostache, R., Schumann, G., Puech, C., Matgen, P., Hoffmann, L. and Pfister, L., 2007. Water level estimation and uncertainty reduction in hydraulic model calibration using satellite SAR images of floods. In: *Proceedings of the 5th International Symposium on Retrieval of Bio– and Geophysical Parameters from SAR Data for Land Applications*, Bari, Italy, 25-28 September 2007. 4

Matgen, P., Henry, J.-B., Pappenberger, F., de Fraipont, P., Hoffmann, L. and Pfister, L., 2004. Uncertainty in calibrating flood propagation models with flood boundaries derived from synthetic aperture radar imagery. In: *Proceedings of the 20th Congress of the International Society of Photogrammetry and Remote Sensing*, Istambul, Turkey, pp. 352–358. 1, 3

Matgen, P., Schumann, G., Pappenberger, F. and Pfister, L., 2007. Sequential assimilation of remotely sensed water stages in flood inundation models. *Remote Sensing for Environmental Monitoring and Change Detection . (Proceedings of Symposium HS3007 at IUGG2007, Perugia, July 2007), IAHS Publ.)*. 6

Pappenberger, F., Beven, K., Horritt, M. and Blazkova, S., 2005. Uncertainty in the calibration of effective roughness parameters in HEC-RAS using inundation and downstream level observations. *Journal of Hydrology* 302(1-4), pp. 46–69. 1

Raclot, D. and Puech, C., 2003. What does AI contribute to hydrology? Aerial photos and flood levels. *Applied Artificial Intelligence* 17(1), pp. 71–86. 1, 3, 5, 6

Roux, H. and Dartus, D., 2006. Use of parameter optimization to estimate a flood wave: Potential applications to remote sensing of rivers. *Journal of Hydrology* 328(1-2), pp. 258–266. 3

Schumann, G., Cutler, M., Black, A., Matgen, P., Pfister, L., Hoffmann, L. and Pappenberger, F., In Press. Evaluating uncertain flood inundation predictions with uncertain remotely sensed water stages. *Journal of River Basin Management*. 1, 4

Schumann, G., Hostache, R., Puech, C., Hoffmann, L., Matgen, P., Pappenberger, F. and Pfister, L., 2007. High-resolution 3D flood information from radar imagery for flood hazard management. *IEEE Transactions on Geoscience and Remote Sensing* 45(6), pp. 1715–1725. 1, 2, 5, 6

Schumann, G., Pappenberger, F. and Matgen, P., submitted. Estimating uncertainty associated with water stages from a single SAR image using a stepped GLUE approach. *Advances in Water Resources*. 3, 6

Smith, L. C., 1997. Satellite remote sensing of river inundation area, stage and discharge : a review. *Hydrological Processes* 11, pp. 1427–1439. 1, 2, 5

United States Army Corps of Engineers (USACE), 2002. Theoretical basis for one-dimensional flow calculations. In: *Hydraulic reference manual*, USACE, Davis (CA, USA), chapter 2. Version 3.1. 3